

## Comparison of robust control methods performance in the UPFC controllers design

Mehdi Nikzad, Shoorangiz Shams Shamsabad Farahani, Mehdi Ghasemi Naraghi, Mohammad Bigdeli Tabar and Ali Javadian

Department of Electrical Engineering, Islamic Azad University, Islamshahr Branch, Tehran, P. O. Box 3135-369, Iran  
Mehdi.nikzad@yahoo.com, Shoorangiz\_shams@yahoo.com, ghasemi@iiu.ac.ir, bigdeli@iiu.ac.ir, javadian@ieee.org

### Abstract

The Unified Power Flow Controller (UPFC) integrates properties of shunt and series compensations and can effectively alters power system parameters in a way that increases power transfer capability and stabilizes system. Simple Proportional-Integral (PI) controllers are applied to UPFC as usual controllers, but parameters of PI controllers are usually tuned based on the trial-and-error approaches and they are incapable to obtain a good dynamic performance under a wide range of operating conditions. To solve this problem, robust control methods are proposed to design UPFC controllers. Also a supplementary damping controller to increase damping of power system oscillations is developed. A Single-Machine Infinite Bus (SMIB) power system installed with a UPFC with system parametric uncertainties is considered as case study. The system parametric uncertainties are obtained by 40% changing parameters from their typical values. Proposed methods are compared with each other to show their effectiveness and robustness. The objectives are to study and comparison robust control methods performance for UPFC control problem.

**Keywords:** Flexible AC Transmission Systems, Unified Power Flow Controller,  $\mu$ -synthesis,  $H_\infty$  loop-shaping

### Nomenclature

FACTS devices: Flexible AC Transmission Systems devices;;UPFC: Unified Power Flow Controller;;QFT method: Quantitative Feedback Theory method; SMIB power system: Single-Machine Infinite Bus power system; SISO system: Single Input - Single Output system; MISO system: Multi Input - Single Output system; MIMO system: Multi input - Multi Output system;  $\omega$ : Synchronous speed of the system;  $\delta$ : Torque angle;  $P_m$ : Mechanical input power;  $P_e$ : Electrical output power;  $M$ : Equivalent inertia of the system;  $D$ : Mechanical damping coefficient;  $E_q'$ : Voltage behind the transient reactance;  $E_q$ : Internal voltage of armature (synchronous generator);  $E_{fd}$ : Internal voltage of armature (synchronous generator);  $T_{do}$ : Open circuit-transient time constant of d axis;  $K_a$ : Gain of voltage regulator;  $T_a$ : Time constant of voltage regulator;  $V_{ref}$ : Reference voltage of voltage regulator;  $V_i$ : Generator terminal voltage;  $V_{dc}$ : DC-link voltage;  $C_{dc}$ : DC-link capacitor;  $m_E$ : Pulse width modulation index of shunt inverter;  $\delta_E$ : Phase angle of the shunt inverter voltage;  $m_B$ : Pulse width modulation index of series inverter;  $\delta_B$ : Phase angle of the series inverter voltage;  $I_{Ed}$ : d-axis current of UPFC;  $I_{Eq}$ : q-axis current of UPFC;  $K_{ij}$ : System constant coefficients;  $T_m$ : Mechanical input torque;  $T_e$ : Electrical output torque;  $\Delta$ : Deviation from nominal value;  $\omega_0$ : Initial value of speed;  $\delta_0$ : Initial value of torque angle;  $\Delta P_{e2ref}$ : reference point of the power of line 2;  $P_{e2}$ : the power of line 2.

### Introduction

The Flexible AC Transmission Systems (FACTS) based on power electronic offer an opportunity to enhance controllability, stability, and power transfer capability of power systems (Hingorani *et al.*, 2000). The Unified Power Flow Controller (UPFC) which is the most versatile FACTS device, has the capabilities of controlling power flow in the transmission lines, improving the transient stability, mitigating system oscillations and providing voltage support (Alawami, 2007; Guo *et al.*, 2009; Jiang *et al.*, 2010; Zarghami *et al.*, 2010).

PID controller is the most commonly used control algorithm in the industry systems, also this technique has been used for FACTS devices control (Ni *et al.*, 1998). The nonlinear natures as uncertainties which exist in the system make it difficult to design an effective controller for the FACTS devices which guarantees fast and stable response under all operating conditions. To deal with such a problem an uncertain model should be considered instead of using a single model plant. This problem has led to study of robust control methods for FACTS devices control (Taher *et al.*, 2008; Taher *et al.*, 2009; Taher *et al.*, 2010).

The objective of this paper is to investigate UPFC

control problem for a Single-Machine Infinite-Bus (SMIB) power system installed with a UPFC with taking into account the uncertainties. In this paper robust control methods such as Quantitative Feedback Theory (QFT) method (Houpis *et al.*, 1999),  $\mu$ -synthesis and  $H_\infty$  loop-shaping (Skogestad *et al.*, 1996) are applied to design UPFC controllers (power-flow controller and DC-voltage regulator). To show effectiveness of robust control methods, they are compared with each other. Simulation results show that the robust controllers guarantee robust performance under a wide range of operating conditions.

### System under study

Fig. 1 shows a SMIB power system installed with UPFC (Hingorani *et al.*, 2000). The UPFC is installed in one of the two parallel transmission lines. This configuration (comprising two parallel transmission lines) permits to control of real and reactive power flow through a line.

### Dynamic model of the system with UPFC

#### Non-linear dynamic model

A non-linear dynamic model of the system is derived by disregarding the resistances of all components of the system (generator, transformers, transmission lines and shunt and series converters) and the transients of the

transmission lines and transformers of the UPFC (Nabaviniaki *et al.*, 1996; Wang, 2000). The nonlinear dynamic model of the system installed with UPFC is given as (1).

$$\begin{cases} \dot{\omega} = \frac{(P_m - P_e - D\Delta\omega)}{M} \\ \dot{\delta} = \omega_0(\omega - 1) \\ \dot{E}'_q = \frac{(-E_q + E_{fd})}{T'_{do}} \\ \dot{E}'_{fd} = \frac{-E_{fd} + K_a(V_{ref} - V_t)}{T_a} \\ \dot{V}_{dc} = \frac{3m_B}{4C_{dc}}(\sin(\delta_E)I_{Ed} + \cos(\delta_E)I_{Eq}) + \frac{3m_B}{4C_{dc}}(\sin(\delta_B)I_{Bd} + \cos(\delta_B)I_{Bq}) \end{cases} \quad (1)$$

The equation for real power balance between the series and shunt converters is given as (2).

$$\text{Re}(V_B I_{B^*}^* - V_E I_E) = 0 \quad (2)$$

**Linear dynamic model**

A linear dynamic model is obtained by linearizing the non-linear dynamic model around the nominal operating condition. The linearised model of the system is given as (3) (Nabaviniaki *et al.*, 1996; Wang, 2000).

$$\begin{cases} \Delta\dot{\delta} = \omega_0\Delta\omega \\ \Delta\dot{\omega} = \frac{-\Delta P_e - D\Delta\omega}{M} \\ \Delta\dot{E}'_q = (-\Delta E_q + \Delta E_{fd})/T'_{do} \\ \Delta\dot{E}'_{fd} = -\left(\frac{1}{T_a}\right)\Delta E_{fd} - \left(\frac{K_a}{T_a}\right)\Delta V \\ \Delta\dot{V}_{dc} = K_7\Delta\delta + K_8\Delta E'_q - K_9\Delta V_{dc} + K_{cc}\Delta m_E + K_{c\delta E}\Delta\delta_E + K_{cb}\Delta m_B \end{cases} \quad (3)$$

Fig. 2 shows the transfer function model of the system including UPFC. The model has constant parameters denoted by  $K_{ij}$ . These parameters are functions of the system parameters and the initial operating condition. Also the control vector  $U$  in Fig. 2 is defined as (4).

$$U = [\Delta m_E \quad \Delta\delta_E \quad \Delta m_B \quad \Delta\delta_B]^T \quad (4)$$

The series and shunt converters are controlled in a coordinated manner to ensure that the real power output of the shunt converter is equal to the power input to the series converter. The fact that the DC-voltage remains constant ensures that this equality is maintained.

**Dynamic model in the state-space form**

The dynamic model of the system in the state-space form is obtained as (5) (Nabaviniaki *et al.*, 1996; Wang, 2000).

$$\begin{bmatrix} \Delta\dot{\delta} \\ \Delta\dot{\omega} \\ \Delta\dot{E}'_q \\ \Delta\dot{E}'_{fd} \\ \Delta\dot{V}_{dc} \end{bmatrix} = \begin{bmatrix} 0 & \omega_0 & 0 & 0 & 0 \\ -\frac{K_1}{M} & 0 & \frac{K_2}{M} & 0 & \frac{K_{pd}}{M} \\ \frac{K_3}{T'_{do}} & 0 & \frac{K_4}{T'_{do}} & \frac{1}{T'_{do}} & \frac{K_{qd}}{T'_{do}} \\ \frac{K_5 K_a}{T_a} & 0 & \frac{K_6 K_a}{T_a} & \frac{1}{T_a} & \frac{K_7 K_a}{T_a} \\ \frac{K_8}{K_9} & 0 & \frac{K_{cc}}{K_9} & 0 & -K_9 \end{bmatrix} \begin{bmatrix} \Delta\delta \\ \Delta\omega \\ \Delta E'_q \\ \Delta E_{fd} \\ \Delta V_{dc} \end{bmatrix} + \begin{bmatrix} 0 & 0 & 0 & 0 \\ \frac{K_{pc}}{M} & \frac{K_{pe}}{M} & \frac{K_{pb}}{M} & \frac{K_{pb}}{M} \\ \frac{K_{qe}}{T'_{do}} & \frac{K_{qe}}{T'_{do}} & \frac{K_{qb}}{T'_{do}} & \frac{K_{qb}}{T'_{do}} \\ \frac{K_{ce}}{T_a} & \frac{K_{ce}}{T_a} & \frac{K_{cb}}{T_a} & \frac{K_{cb}}{T_a} \\ \frac{K_{cc}}{K_9} & \frac{K_{c\delta E}}{K_9} & \frac{K_{cb}}{K_9} & \frac{K_{cb}}{K_9} \end{bmatrix} \begin{bmatrix} \Delta m_E \\ \Delta\delta_E \\ \Delta m_B \\ \Delta\delta_B \end{bmatrix} \quad (5)$$

The typical values of the system parameters for the nominal operating condition are given in appendix. The

system parametric uncertainties are obtained by 40% changing load (active and reactive powers) from their nominal values. Regarding these uncertainties, six operating conditions are defined and shown in appendix.

**UPFC control strategy**

The UPFC control strategy comprises three controllers as: i. Power flow controller, ii. DC-voltage regulator and iii. Power system oscillations-damping controller.

**Power flow controller and DC-voltage regulator**

The UPFC is installed in one of the two lines of the SMIB power system. The power flow controller regulates the power flow on transmission line. Power flow is regulated by modulating the pulse width modulation index  $m_B$  of series inverter. Also the real power output of the shunt converter should be equal to the real power input of the series converter or vice versa. In order to maintain the power balance between the two converters, a DC-voltage regulator is incorporated. DC-voltage is regulated by modulating the phase angle of the shunt converter voltage.

*Power system oscillations-damping controller*

A damping controller is provided to improve the damping of power system oscillations. This controller may be considered as a lead-lag compensator (Yu, 1983). However an electrical torque ( $\Delta T_m$ ) in phase with the speed deviation ( $\Delta\omega$ ) should be produced in order to improve damping of power system oscillations.

**Analysis**

For the nominal operating condition the eigenvalues of the system are obtained using

*Table 1. Eigen-values of the closed-loop system without damping controller*

-19.2516
+0.0308 ± 2.8557i
-0.6695 ± 0.5120i

state-space model of the system presented in (5) and these eigen values are shown in Table 1. It is clearly seen that the system is unstable and needs to power system stabilizer (damping controller) for stability.

**Damping controller design for stability**

The damping controllers are designed to produce an electrical torque in phase with the speed deviation according to phase compensation method (Yu, 1983). The four control parameters of the UPFC ( $m_B$ ,  $m_E$ ,  $\delta_B$  and  $\delta_E$ ) can be modulated in order to produce the damping torque. In this paper  $m_B$  is modulated in order to damping controller design. The speed deviation  $\Delta\omega$  is considered as the input to the damping controller. The structure of a typical damping controller is as follows:

$$U = K_{DC} \frac{ST_W}{1 + ST_W} \frac{1 + ST_1}{1 + ST_2} \Delta\omega \quad (6)$$

It consists of gain ( $K_{DC}$ ), signal washout ( $T_w$ ) and phase compensator block parameters ( $T_1$  and  $T_2$ ). The parameters of the damping controller are obtained using the phase compensation technique. The detailed step-by-step procedure for computing the parameters of the

damping controller using phase compensation technique is presented in (Yu, 1983). Damping controller based  $m_B$  has been designed and obtained as follow:  $K_{DC}=417.5$ ,  $T_W=10$ ,  $T_1=4.7$ ,  $T_2=5.566$ . The eigenvalues of the system with damping controller are obtained and listed in Table 2 and it is clearly seen that the system is stable.

Table 2. Eigen-values of the closed-loop system containing damping controller

-19.3328
-16.4275
-3.8609
-0.8814
-0.1067
$-0.9327 \pm 0.8437i$

This equation is used to define the desired fixed point mapping where each of the 4 matrix elements on the right side of this equation can be interpreted as a MISO problem. Proof of the fact that design of each MISO system yields a satisfactory MIMO design is based on the schauder fixed point theorem (Houpis *et al.*, 1999).

### Problem specification

After system stabilization by applying the damping controller, The UPFC controllers (power-flow controller and DC-voltage regulator) are simultaneously designed based on the robust control technique. Since two controllers should be simultaneously designed, therefore the problem is a  $2 \times 2$  MIMO problem and the design technique for MIMO systems should be considered. Since controller design for MIMO systems is a sophisticated procedure, so in first the MIMO system is converted to equivalent MISO systems and then controllers are designed for these MISO systems. Using fixed point theory (Houpis *et al.*, 1999) a  $2 \times 2$  MIMO system can be decentralized into 2 equivalent single-loops MISO systems (2 inputs and one output). Each MISO system design is based upon the specifications relating its output and all of its inputs. The basic MIMO compensation structure for a  $2 \times 2$  MIMO system is shown in Fig. 3. That consists of the uncertain plant matrix  $P(S)$  and the diagonal compensation matrix  $G(S)$ . These matrices are defined as (7).

$$\begin{cases} P(s) = [P_{ij}(s)] = \begin{bmatrix} P_{11} & P_{12} \\ P_{21} & P_{22} \end{bmatrix} \\ G(s) = \text{diag}\{G_i(s)\} = \begin{bmatrix} G_1 & 0 \\ 0 & G_2 \end{bmatrix} \end{cases} \quad (7)$$

Fixed point theory develops a mapping that permits the analysis and synthesis of a MIMO control system by a set of equivalent MISO control systems. For  $2 \times 2$  system, this mapping results in 2 equivalent systems, each with two inputs and one output. One input is designated as a desired input and the other as a disturbance input. The inverse of the plant matrix is represented by (8).

$$P(s)^{-1} = \begin{bmatrix} P^*_{11} & P^*_{12} \\ P^*_{21} & P^*_{22} \end{bmatrix} \quad (8)$$

The effective plant transfer functions are formed as follows:

$$Q = \begin{bmatrix} q_{11} & q_{12} \\ q_{21} & q_{22} \end{bmatrix} = \begin{bmatrix} \frac{1}{P^*_{11}} & \frac{1}{P^*_{12}} \\ \frac{1}{P^*_{21}} & \frac{1}{P^*_{22}} \end{bmatrix} \quad (9)$$

Based on the above discussions, in this study the UPFC control problem specifications given as: The controllers: power flow controller and DC-voltage regulator; Number of controllers: 2 controllers; Plant matrix  $P(S)$  is a  $2 \times 2$  matrix; Diagonal compensation matrix  $G$  contains two compensators  $G_1$  and  $G_2$ .

Using dynamic state-space model of the SMIB power system presented in (5), the plant transfer function matrix  $P(S)$  is obtained with the related inputs and outputs which have been shown in Fig. 4. Where, the  $P(S)$  is uncertain plant transfer function of the system and it is clear that the  $P(S)$  is a  $2 \times 2$  matrix. The structure of the control loop can be shown as Fig. 4.

Where, the  $P(S)$  is obtained using the state space model of the system presented in (5) at all operating conditions. The compensators  $G_1$  and  $G_2$  are designed so that the variations of  $P_{e2}$  and  $V_{DC}$  (system outputs) be within the acceptable range under all operating conditions.

The system operating conditions have been defined in appendix. According to these operating conditions and plant transfer function for any operating condition, the effective plant transfer functions defined in (9) ( $q_{11}$  and  $q_{22}$ ) are obtained at any operating condition. Then, according to fixed point theory, power flow controller ( $G_1$ ) is designed based on the effective plant transfer function  $q_{11}$  and DC-voltage regulator ( $G_2$ ) is designed based on the effective plant transfer function  $q_{22}$ . In fact the MIMO problem is converted to two MISO problems. In the next part, the controller design process for these MISO systems is proposed using robust control methods.

### UPFC controllers design

In this investigation three robust control methods are applied to design UPFC controllers (power flow controller and DC-voltage regulator). These approaches are developed in continue.

#### UPFC controllers design using QFT method

Quantitative Feedback Theory (QFT) is a unified theory that emphasizes to use of feedback for achieving the desired system performance tolerances despite plant uncertainty and plant disturbances. QFT quantitatively formulates these two factors are: (i)- Sets  $\tau_R = \{T_R\}$  of acceptable command or tracking input-output relations and sets  $\tau_D = \{T_D\}$  of acceptable disturbance input-output relations and (ii)- Sets  $\rho = \{P\}$  of possible plants.

The object is to guarantee that the control ratio (system transfer function)  $T_R = Y/R$  is a member of  $\tau_R$

Fig.1. A single machine Infinite bus (SMIB) power system installed with UPFC in one of the lines

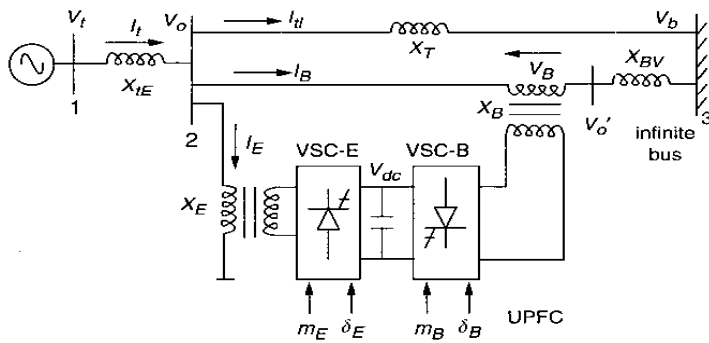


Fig.3. The control structure for a 2x2 MIMO system

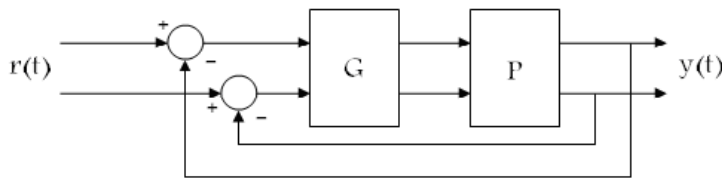


Fig. 4. Closed-loop system for power-flow controller and DC-Voltage regulator

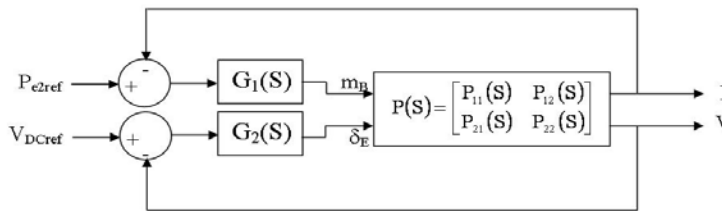


Fig. 5. Structure of closed-loop system for power-flow control

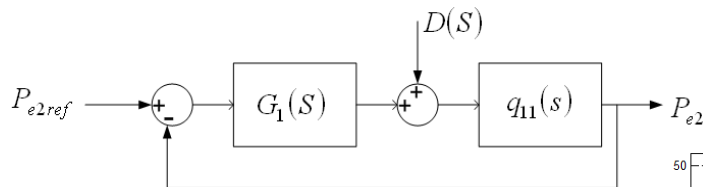


Table 3. Performance index following 5% step change in the reference mechanical torque ( $\Delta T_m$ )

	Performance Index		
	$H_\infty$	-synthesis $\mu$	QFT
Operating condition 1	0.0299	0.0283	0.0274
Operating condition 2	0.0325	0.0309	0.0288
Operating condition 3	0.0332	0.0324	0.0317
Operating condition 4	0.0345	0.0333	0.0330
Operating condition 5	0.0389	0.0352	0.0341
Operating condition 6	0.0312	0.0302	0.0281

Fig.2. Transfer function model of the system including UPFC

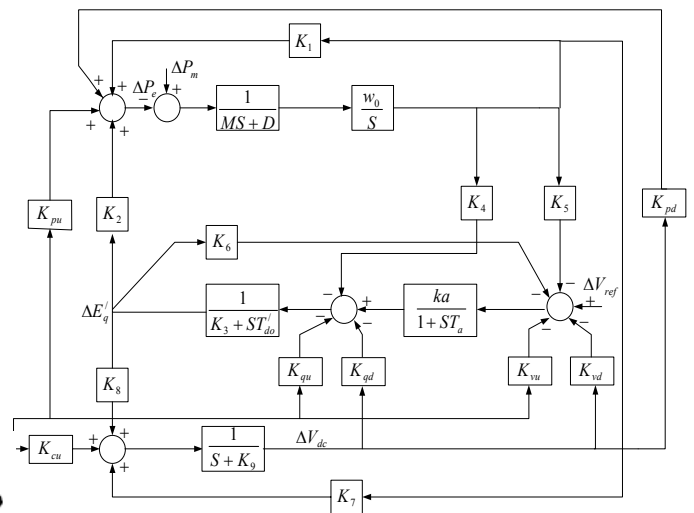


Fig. 6. Templates of effective plant transfer function  $q_{11}$

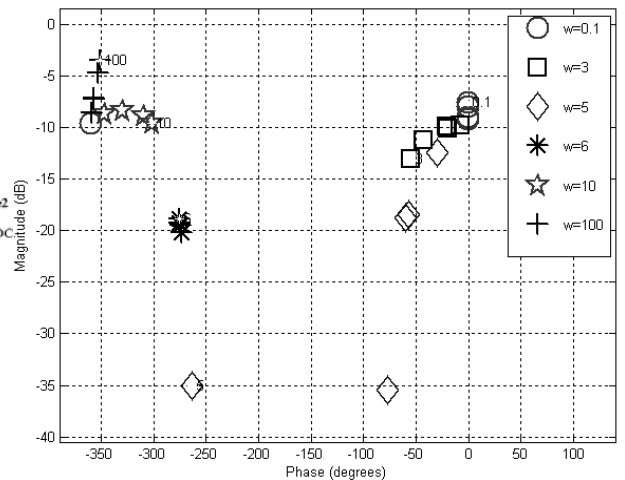
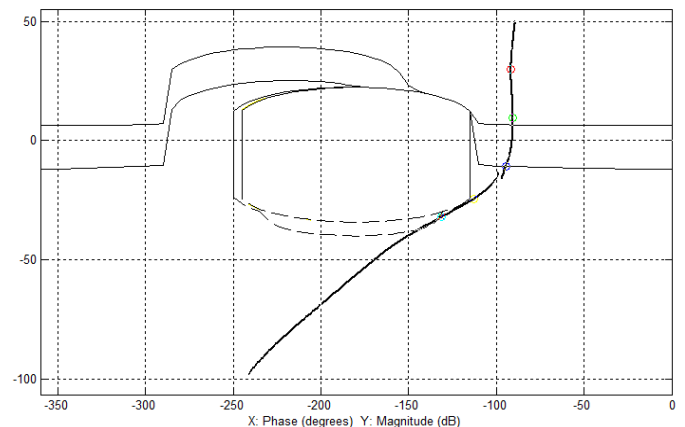


Fig. 7. Bounds and loop shaping for  $q_{11}$



and  $T_D=Y/D$  is a member of  $\tau_D$  for all  $P(S)$  in  $p$ . QFT is essentially a frequency-domain technique and in this paper is used for multiple input - single output (MISO) systems. It is possible to convert the MIMO system into its equivalent sets of MISO systems to which the QFT design technique is applied. The objective is to solve the MISO problems, for example to find compensation functions which guarantee that the performance tolerance of each MISO problem is satisfied for all  $P$  in  $p$ . The QFT technique is completely developed in (Houpis *et al.*, 1999).

**Power flow controller design using QFT method:** Based on the discussions in the section 6, the structure of control system for power flow controller is shown in Fig. 5. It can be clearly seen that the system is a MISO system and the compensator  $G_1$  will be designed based on  $q_{11}$  (Taher *et al.*, 2009).

Based QFT technique, the first step in the design process is to plot the plant uncertainties in the Nichols diagram. This plot is referred to as system templates. The Templates of  $q_{11}$  are obtained in some frequencies and shown in Fig. 6.

Compensator  $G_1$  is designed so that the variation of output response ( $P_{e2}$ ) be within the acceptable range under all uncertainties of  $q_{11}$  and all operating conditions. Next step in design of  $G_1$  is to define tracking bounds for output response. In this problem the desired upper and lower bounds for output response are considered as (10).

$$\text{lower\_bound} = \frac{15}{s^3 + 60.9s^2 + 54.25s + 15} \quad (10)$$

$$\text{upper\_bound} = \frac{0.81S + 24.3}{30S^2 + 37.8S + 24.3}$$

The output response (transmission power of line 2) is acceptable if it lies between the desired upper and lower bounds or in the other word the output response should track input response with specified characteristics in tracking bounds. Next step in QFT design process is to obtain tracking bounds. Using templates and defined upper and lower bounds the tracking bounds are obtained based on QFT technique. In this plant since system characteristics are tracking, therefore it is not necessary to consider disturbance rejection bounds. Thus the tracking bounds ( $B_R(j\omega)$ ) are considered as composite bounds ( $B_O(j\omega)$ ). Also minimum damping ratios  $\xi$  for the dominant roots of the closed-loop system is considered as  $\xi=1.2$  and this amount on the Nichols chart establishes a region which must not be penetrated by the template of loop shaping ( $L_O$ ) for all frequencies. The boundary of this region is referred to as U-contour. U-contour and the composite bound ( $B_O(j\omega)$ ) and an optimum loop shaping ( $L_{O1}$ ) based these bounds are shown in Fig. 7. Using  $L_{O1}$  the compensator  $G_1$  is obtained as follow (the order has been reduced by model reduction technique):

$$G_1(s) = \frac{L_{O1}(s)}{q_{11}(s)} \Rightarrow G_1(S) = \frac{34.9129(S+3.299)}{S(S+4.771)(S^2 + 3.932s + 8.401)} \quad (11)$$

**DC-voltage regulator design using QFT method:**

Considering a similar method for DC-voltage regulator design lead to a controller as follow:

$$G_2(s) = \frac{L_{O2}(s)}{q_{22}(s)} = \frac{275.319(S+3.813)(S+0.241)}{S(S+35.36)(S+0.9812)(S^2 + 98.32S + 2381)} \quad (12)$$

**UPFC controllers design using  $H_\infty$  loop-shaping**

In  $H_\infty$  loop shaping technique, the adopted control method is based on  $H_\infty$  robust stabilization combined with classical Loop-shaping, where 'loop-shape' refers to the magnitude of the loop transfer function  $L=GK$  as a function of frequency. It is essential to consider tow-step procedure, where in the first step; the singular values of the open-loop plant are shaped by pre and post compensators. In the second step, the resulting shaped plant is robustly stabilized with respect to co-prime factor uncertainty and using  $H_\infty$  optimization. An important advantage is that no problem-dependent uncertainty modeling or weight selection is required in this second step (Taher *et al.*, 2008). The UPFC power flow controller and DC voltage regulator are independently designed. After trial and error,  $w_1$  and  $w_2$  for power flow controller and DC-voltage regulator are chosen as (Taher *et al.*, 2008). Two controllers which satisfy design objectives are obtained. For easy implementation, the order is reduced by model reduction technique. The transfer functions of the controllers are as follow (Taher *et al.*, 2008):

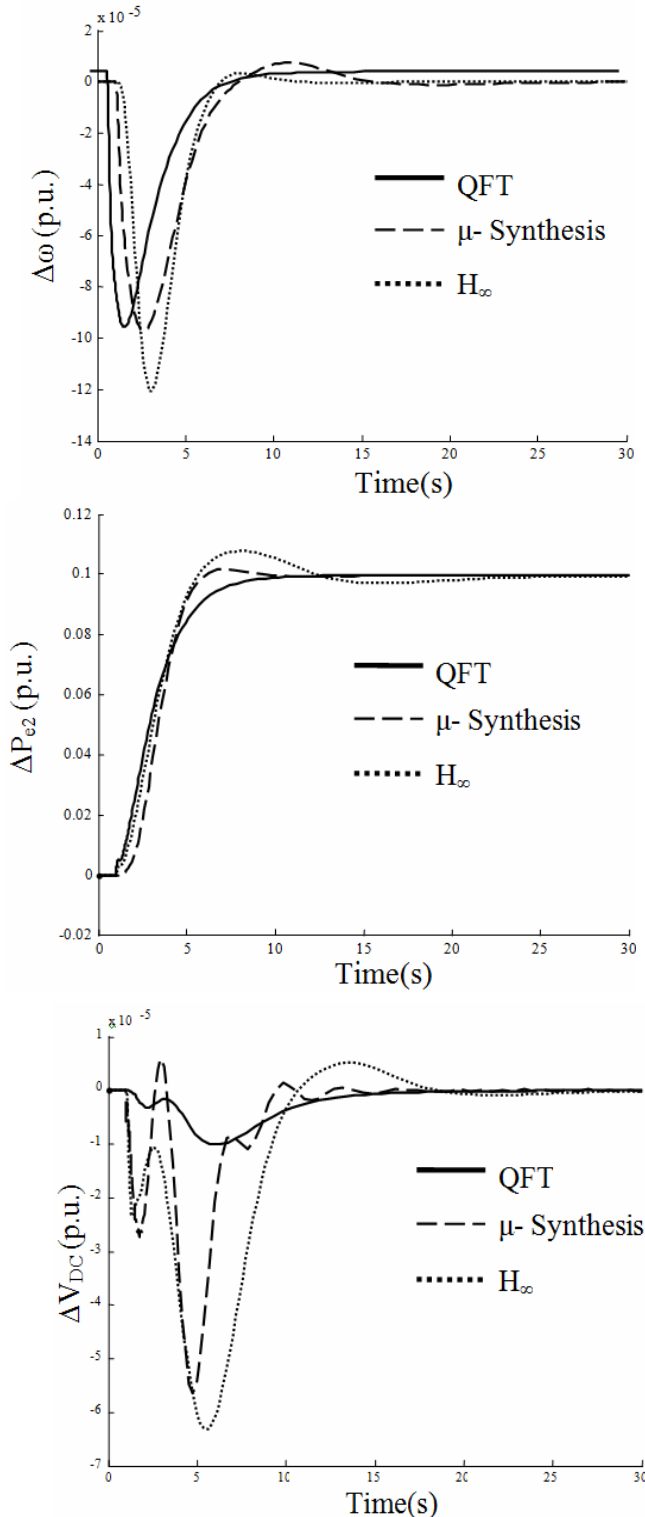
$$G_1 = \frac{0.0284(S+0.0821)(S+0.77)(S^2+1.021S+2.25)}{S(S+14.87)(S^2+0.3192S+0.04109)(S^2+0.894S+2.103)}$$

$$G_2 = \frac{59102(S+18.28)(S^2+2.149S+1.647)}{S(S+5230)(S+51.31)(S+8.773)(S^2+211.912S+1829.012)} \quad (13)$$

**UPFC controllers design using  $\mu$ -synthesis**

The structured singular value ( $\mu$ ) is an appropriate tool for analyzing the robustness and synthesizing a system which is subjected to structured Linear Fraction Transformers (LFT). The detailed step-by-step procedure for computing the controllers using structured singular value ( $\mu$ -based) technique is given in (Taher *et al.*, 2010). For robust control design, an open loop system is represented by nominal plant model  $P_{nom}(s)$  and the uncertainty set which covers the differences between  $P_{nom}(s)$  and the actual system. This uncertainty set represents the unstructured uncertainty of the system using frequency-domain bounds on transfer functions. The model uncertainty percentage is represented by the weights  $W_{upe}$  and  $W_{uvdc}$  which corresponds to the frequency variations of the model uncertainty. These weighting functions are chosen to cover the maximum uncertainty as (Taher *et al.*, 2010). To guarantee the robust performance and satisfy the control objectives, it is need to add a fictitious uncertainty block to each control loop  $P_{e2}$  and  $V_{dc}$ . This fictitious uncertainty block must be along with the corresponding performance weights ( $W_C$  and  $W_P$ ) and associated with the control effort and control error minimization, respectively.

Fig. 8. Dynamic responses at nominal load (operating condition 1), following 0.1 step change in the reference power of line 2 ( $\Delta P_{e2(ref)}$ ) a: Dynamic response  $\Delta\omega$  b: Dynamic response  $\Delta P_{e2}$  c: Dynamic response  $\Delta V_{DC}$



The weight  $W_d$  is normalized at the input disturbances and the weight  $W_n$  is normalized at the input noise. To

keep the controller complexity low, the order of selected weights should be kept low. More details about choosing weights are given in (Taher *et al.*, 2010). Suitable set of weighting functions for  $P_{e2}$  and  $V_{dc}$  are chosen as (Taher *et al.*, 2010). The robust synthesis problem is obtained in terms of the  $\mu$ -theory and the  $\mu$ -analysis and synthesis toolbox is used to obtain optimal controller (Taher *et al.*, 2010). The transfer functions of the reduced order controllers are given as follows:

$$G_1 = 0.049 \frac{(S + 221.87)(S + 3.415)(S + 0.2891)}{S(S + 3.496)(S + .1491)}$$

$$G_2 = 1129.34 \frac{(S + 3.25)(S^2 + 0.709S + 3.991)(S^2 + 1.218S + 2.903)}{S(S + 12.8)(S + 1.031)(S^2 + 3.741S + 205.41)} \quad (14)$$

**Simulation results**

The classical method to compare responses is to show responses following step change at inputs. The responses  $\Delta P$ ,  $\Delta\omega$  and  $\Delta V_{DC}$  should be showed to comparison purposes. Since showing many figures is not favorable, so a performance index can be considered for more comparison purposes. Here, the performance index is defined as follow:

$$\text{Performance index} = \int_0^t |\Delta\omega| dt + \int_0^t |\Delta V_{DC}| dt + \int_0^t |\Delta P_{e2}| dt \quad (15)$$

In fact the performance index is the total area under the curves (output responses) and this performance index is a suitable benchmark to compare performance of robust controllers with each other. The parameter "t" in performance index is the simulation time and considered from zero to settling time of response. It is clear to understand that the controller with lower performance index is better than the other controllers or on the other words the controller with lower performance index has better performance than the other controllers. The performance index has been calculated following 5% step change in the reference mechanical torque ( $\Delta T_m$ ) in several operating conditions (The operating conditions have been given in appendix). The result is given at Table 3. It is clear to see that QFT controllers have better performance than the other controllers at all operating conditions. QFT controllers have lower performance index in comparison with the other controllers and therefore the QFT controllers can mitigate power system oscillations successfully. After QFT the  $\mu$ -synthesis method can be considered as second method and  $H_\infty$  method is a poor method in comparison with the other methods. Although the table result is enough to compare robust methods, but it can be useful to show responses in figure.

Fig.8 shows the dynamic responses for a 10% step change in the reference power of line 2 ( $\Delta P_{e2(ref)}$ ) with  $\mu$  synthesis,  $H_\infty$  and QFT controllers. This figure shows that all proposed methods have an excellent capability in damping of power system oscillations and also power system stability enhancement under small disturbances. But between these methods, the QFT controllers have the

best performance in power transmission tracking and damping of power system oscillations in comparison with  $\mu$ -synthesis and  $H_{\infty}$  controllers. With QFT controllers the power transmission of line 2 changes to 0.1 (value of input step) and also DC-voltage is driven back to zero after 0.1 step change in the reference power of line 2. Also between  $\mu$ -synthesis and  $H_{\infty}$  controllers, the  $\mu$ -synthesis controllers have better performance than  $H_{\infty}$  controllers. Eventually according to simulation results the  $H_{\infty}$  method has a poor performance in comparison with the other methods. Also QFT controllers are more low order than the other controllers.

Table 4. The nominal system parameters

$X_d = 1$ p.u.	$T'_{do} = 5.044$ s	$M = 8$ Mj/MVA	Generator
$D = 0$	$X'_d = 0.3$ p.u.	$X_q = 0.6$ p.u.	
$T_a = 0.05$ s	$K_a = 10$		Excitation system
$X_{SDT} = 0.1$ p.u.	$X_{te} = 0.1$ p.u.		Transformers
$X_{T2} = 1.25$ p.u.	$X_{T1} = 1$ p.u.		Transmission lines
$Q = 0.16$ p.u.	$P = 0.82$ p.u.	$V_t = 1.032$ p.u.	Operating condition
$C_{DC} = 3$ p.u.	$V_{DC} = 2$ p.u.		DC link parameters
$m_B = 0.104$ $\delta_B = -55.87^\circ$	$m_E = 1.0378$ $\delta_E = 29.46^\circ$		UPFC parameters

### Conclusion

In this paper a robust decentralized UPFC controller design based on robust control methods was proposed. The three robust methods considered and applied to design controllers are QFT,  $\mu$ -synthesis and  $H_{\infty}$ . These design strategies include enough flexibility to set the desired level of stability and performance and consider the practical constraints by introducing appropriate uncertainties. The proposed methods were applied to a typical SIMB power system installed with UPFC with system parametric uncertainties and various load conditions. The simulation results demonstrated that the designed controllers were able to guarantee the robust stability and robust performance under a wide range of parametric uncertainties and load conditions. Also, simulation results showed that these methods are robust to change in the system parameters. All the proposed methods have an excellent capability in damping of power system oscillations and enhance power system stability. But between robust control methods, QFT method has the best performance in power system control and damping oscillations. After QFT method, between  $\mu$ -synthesis and  $H_{\infty}$  methods, the former has more ability to set the desired level of stability and performance than the latter and can be considered as the

Table 5. System operating conditions

$V_t = 1.032$ p.u.	$Q = 0.16$ p.u.	$P = 0.8$ p.u.	Operating condition 1
$V_t = 1.032$ p.u.	$Q = 0.17$ p.u.	$P = 0.90$ p.u.	Operating condition 2
$V_t = 1.032$ p.u.	$Q = 0.20$ p.u.	$P = 1.00$ p.u.	Operating condition 3
$V_t = 1.032$ p.u.	$Q = 0.28$ p.u.	$P = 1.10$ p.u.	Operating condition 4
$V_t = 1.032$ p.u.	$Q = 0.30$ p.u.	$P = 1.12$ p.u.	Operating condition 5
$V_t = 1.032$ p.u.	$Q = 0.10$ p.u.	$P = 0.70$ p.u.	Operating condition 6

second method for UPFC controllers design. Eventually the  $H_{\infty}$  is a poor method in comparison to the other methods.

### Appendix

The nominal parameters and operating conditions of the system are listed in Table 4. The uncertainty areas for active and reactive powers are defined as follow:  $0.7 \leq P \leq 1.125$  and  $0.1 \leq Q \leq 0.3$ . The operating conditions are listed in Table 5. Where, the operating condition 1 is the nominal operating condition.

### References

- Alawami T (2007) A particle-swarm-based approach of power system stability enhancement with UPFC. *Electrical Power and Energy Systems*. 29, 251-259.
- Guo J, Crow ML and Sarangapani J (2009) An improved UPFC control for oscillation damping. *IEEE Transactions on Power Systems*. 25 (1), 288 - 296.
- Hingorani NG and Gyugyi L (2000) Understanding FACTS. *IEEE Press*, NY.
- Houpis CH and Rasmussen SJ (1999) Quantitative feedback theories fundamental and applications. *Marcel Dekker Inc*. NY, Basel.
- Jiang X, Chow JH, Edris A and Fardanesh B (2010) Transfer path stability enhancement by voltage-sourced converter-based FACTS controllers. *IEEE Transactions on Power Delivery*. 25 (2), 1019 - 1025.
- Nabaviniaki A, Iravani MR (1996) Steady-state and dynamic models of Unified Power Flow Controller for power system studies. *IEEE Transactions on Power Systems*. 11 (4), 1937-1950.
- Ni Y, Jiao L, Chen S and Zhang B (1998) Application of a nonlinear PID controller on STATCOM with a differential tracker. *International Conference on Energy Management and Power Delivery*. NY, USA, 29-34.
- Skogestad S and Postlethwaite I (1996) Multivariable feedback control. John Wiley.
- Taher SA, Akbari SH, Abdoalipour A and Hematti R (2008) Design of robust UPFC controllers using  $H_{\infty}$  control theory in electric power system. *Am. J. Appl. Sci*. 5 (8), 980-989.
- Taher SA, Akbari SH, Abdoalipour A and Hematti R (2010) Robust decentralized controller design for UPFC controllers using  $\mu$  synthesis. *Commun. in Non Linear Sci. & Numerical Simulation*. 15, 2149-2161.
- Taher SA, Hemati R and Abdolalipour A (2009) UPFC controller design using QFT method in electric power systems. *Intl. IEEE Conf., EUROCON*, Saint Petersburg, Russia.
- Wang HF (2000) A unified model for the analysis of FACTS devices in damping power system oscillations-part III: Unified Power Flow Controller. *IEEE Transactions on Power Delivery*. 5 (3), 978-990.
- Yu YN (1983) Electric power system dynamics. *Acad. Press, Inc.*, London.
- Zarghami M, Crow ML, Sarangapani J, Liu Y and Atcitty S (2010) A novel approach to inter-area oscillations damping by Unified Power Flow Controllers utilizing ultra-capacitors. *IEEE Transactions on Power Systems*. 25 (1), 404 - 412.